Binding of Cytochrome *c* to Liposomes As Revealed by the Quenching of Fluorescence from Pyrene-Labeled Phospholipids

Pekka Mustonen,[‡] Jorma A. Virtanen,[§] Pentti J. Somerharju,[∥] and Paavo K. J. Kinnunen*[,‡]

Departments of Medical Chemistry, Chemistry, and Basic Chemistry, University of Helsinki, Helsinki, Finland

Received July 18, 1986; Revised Manuscript Received January 14, 1987

ABSTRACT: Resonance energy transfer from pyrene–fatty acid containing phospholipid derivatives to the heme of cytochrome *c* (cyt *c*) was used to observe the binding of this protein to liposomal membranes. Liposomes were formed of egg yolk phosphatidic acid (PA) and either egg yolk phosphatidylcholine or dipalmitoylphosphatidylcholine with 1 mol % of the fluorescent lipid. Binding of cyt *c* to liposomes was monitored by measuring the decrease either in the fluorescence intensity or in the lifetime of pyrene emission. The requirement for the presence of the acidic phospholipid in the membrane for the binding of cyt *c* could be reconfirmed. Below 5 mol % of phosphatidic acid in the membrane, no significant attachment of cyt *c* to liquid-crystalline bilayers was evident whereas upon increasing the concentration of PA further the association of cyt *c* progressively increased until a saturation was reached at about 30 mol % of phosphatidic acid. Addition of NaCl caused the fluorescence intensity and lifetimes to return to values observed in the absence of cyt *c*, thus revealing the dissociation of the protein from the membrane. The pyrene-labeled phosphatidic acid derivatives PPHPA and PPDPA were quenched more effectively than the corresponding phosphatidylcholines, apparently due to the direct involvement of the acidic head group in binding cyt *c*. When dipalmitoylphosphatidylcholine (DPPC) with 5 mol % of phosphatidic acid was used, no binding of cyt *c* to the liposomes above the phase transition temperature of the former lipid could be demonstrated whereas below the transition temperature (T_m) binding did take place. This indicates that below T_m phase separation of PA occurs, thus forming negatively charged patches with high enough surface charge density to provide binding sites for cyt *c*. Therefore, such transition-induced phase separation in the membrane lipids could provide a control mechanism for the membrane binding of cyt *c* type peripheral membrane proteins. These data also indicate that the membrane-bound cyt *c* has a long-range ordering effect on the membrane lipids. The membrane microdomains with bound cyt *c* are further suggested to pack into a trigonal superlattice.

Cytochrome *c* is a well-characterized peripheral membrane protein of mitochondria. Binding of cyt *c*[1] to fully hydrated acidic phospholipid containing membranes is mainly electrostatic and is thus sensitive to changes in the ionic strength and pH (Green & Fleischer, 1963; Quinn & Dawson, 1969; Kimelberg & Lee, 1969; Steinemann & Läuger, 1971; Chapman & Urbina, 1971; Vanderkooi et al., 1973; Nicholls et al., 1973; Nicholls, 1974; Van & Griffith, 1975; Brown & Wütrich, 1977a). Phosphatidylcholine vesicles do not bind cyt *c* (Green & Fleischer, 1963; Vanderkooi et al., 1973; Nicholls & Malviya, 1973). Of the negatively charged lipid species, phosphatidic acid provides the binding site with highest affinity (Nicholls & Malviya, 1973). In mixed-lipid membranes containing acidic and zwitterionic phospholipids, cyt *c* has been reported to cause lateral phase separation (Birrell & Griffith, 1976; Brown & Wütrich, 1977b). Binding of cyt *c* to liposomes also increases their solute permeability (Kimelberg & Papahadjopoulos, 1971).

A variety of techniques have been employed to characterize the association of cyt *c* with lipid membranes. One of the most informative is fluorescence resonance energy transfer as the heme moiety can be used as a natural acceptor for suitable donors (Fromherz, 1970; Vanderkooi et al., 1973; Pohl & Teissie, 1975; Faucon et al., 1976; Teissie & Baudras, 1977; Teissie, 1981). Phospholipid derivatives with a covalently coupled pyrene in one or both acyl chains have thus far been used, for instance, to study phase separation and lateral diffusion, as well as conformational alterations and organization of phospholipids in model membranes (Galla & Hartmann, 1977; Sunamoto et al., 1980; Thurén et al., 1984; Somerharju et al., 1985). Here we describe results from the use of pyrene–fatty acid containing phospholipids as quantum donors in Förster-type resonance energy transfer to the heme of cyt *c*.

Materials and Methods

Lipids. Egg PC was isolated according to Singleton et al. (1965). Egg PA was prepared by phospholipase D catalyzed hydrolysis of egg PC (Davidson & Long, 1958). 1-Palmitoyl-2-[10-(pyren-1-yl)decanoyl]-and 1-palmitoyl-2[6-(pyren-1-yl)hexanoyl]-*sn*-glycero-3-phosphocholine (PPDPC and PPHPC, respectively) were purchased from KSV Chemical

* Address correspondence to this author.
‡ Department of Medical Chemistry.
§ Department of Chemistry.
∥ Department of Basic Chemistry.

[1] Abbreviations: cyt *c*, cytochrome *c*; DPPC, 1,2-dipalmitoyl-*sn*-glycero-3-phosphocholine; EDTA, ethylenediaminetetraacetic acid; egg PA, egg phosphatidic acid; egg PC, egg phosphatidylcholine; POPOP, 1,4-bis[2-(5-phenyloxazolyl)]benzene; PPDPA, 1-palmitoyl-2-[10-(pyren-1-yl)decanoyl]-*sn*-glycero-3-phosphatidic acid; PPDPC, 1-palmitoyl-2-[10-(pyren-1-yl)decanoyl]-*sn*-glycero-3-phosphocholine; PPHPA, 1-palmitoyl-2-[6-(pyren-1-yl)hexanoyl]-*sn*-glycero-3-phosphatidic acid; PPHPC, 1-palmitoyl-2-[6-(pyren-1-yl)hexanoyl]-*sn*-glycero-3-phosphocholine; RFI, relative fluorescence intensity; τ, fluorescence lifetime; R-τ, relative τ; T_m, phospholipid phase transition temperature; Tris, tris(hydroxymethyl)aminomethane.

0006-2960/87/0426-2991$01.50/0

Co. (Valimotie 7, Helsinki, Finland). PPDPA and PPHPA were obtained by phospholipase D reaction from the corresponding phosphatidylcholines and were purified by preparative thin-layer chromatography on silicic acid plates (Merck, Darmstadt, FRG) with chloroform/methanol/acetic acid/water (24:15:4:2, by volume) as solvent. DPPC was from Sigma and was used without further purification.

Preparation of Liposomes. The indicated lipids were mixed in chloroform/methanol (3:1, by volume) whereafter the solvents were removed under a stream of nitrogen. After the 0.5 h under reduced pressure, the lipids were hydrated with 20 mM Tris-HCl–1 mM EDTA, pH 7.4. Unless otherwise indicated, the final total concentration of lipid was 0.2 mM. The content of the probe was 1 mol % of the total lipid. To obtain unilamellar vesicles, the dispersions were sonicated under a purge of nitrogen for 5 min in an ice–water bath or for DDPC at 45 °C with a Branson sonifier equipped with a microtip probe and operated at 45-W output. Multilamellar liposomes were prepared by sonication for 40 s with a Branson 220 bath sonicator. In order to produce liposomes intermediate between large multilamellar and small unilamellar vesicles, sonication for 5 min in a Branson horn-type cavity was employed. The purpose of the different sonication procedures was to vary the average dispersive power input on a very crude scale to obtain liposome preparations with different amounts of lipid in the outermost monolayer. Accordingly, the actual sizes of the liposomes were not determined, and the above distinction must essentially be regarded as tentative only. From the point of view of this study, this matter is, however, not of significance.

Fluorescence Spectroscopy. Fluorescence measurements were carried out with an SLM 4800S instrument interfaced to a Hewlett-Packard 85 computer. Excitation was at 343 nm. Emission intensities were measured at 377 nm and the fluorescence lifetimes at 382 nm. The above wavelengths were selected with monochromators. In lifetime measurements, 1- and 8-nm slits were used for excitation and emission beams, respectively. In intensity measurements the corresponding values were 2 and 4 nm. Two milliliters (0.4 μmol of lipid) of the liposome solutions was placed into a magnetically stirred four-window quartz cuvette in a holder thermostated with a circulating water bath. Unless otherwise stated, the experiments were carried out at 25 °C. Aliquots of 1–5 μL of a 0.16 mM solution of cyt *c* (from horse heart, type VI from Sigma, reduced with ascorbate) were added to the liposome solutions. Binding of cyt *c* was rapid, and changes in fluorescence were stabilized within 0.5 min whereafter either the intensity or the lifetime of pyrene monomer fluorescence was determined. To ensure the ionic nature of the attachment of cyt *c* to the liposomes, an aliquot of concentrated NaCl solution was added to the cuvette after the completion of a cyt *c* binding assay. No attempt was made to check the minimal concentration of salt to cause dissociation. To eliminate the influence of Brownian motion, a Glan–Thomson polarizing prism at an angle of 35° was set in the exciting beam (Spencer & Weber, 1970). POPOP was used as a lifetime reference (Lakowicz et al., 1981). Lifetime values from the intensity demodulation were obtained with a modulation frequency of 6 MHz. Each of the values given represents the mean of 200 collected data points. The maximum average error in the measured lifetimes was of the order of ±3%, usually, however, less than 1%. For the sake of clarity, error bars for deviations less than 1.5% are not shown.

Our preliminary measurements on fluorescence decay kinetics of neat Langmuir–Blodgett films of these pyrene-labeled

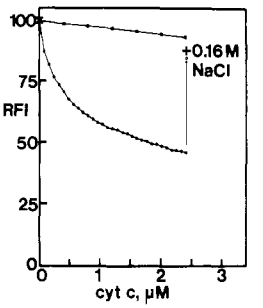

FIGURE 1: Cytochrome *c* induced quenching of the relative fluorescence intensity of pyrene monomer emission (RFI) from PPDPA in egg PC liposomes containing either no egg PA (■) or 20 mol % of the latter lipid (●). In order to reduce the extent of trivial absorption and the amount of scattered light, the total lipid concentration in this experiment was 50 μM. The arrow indicates the effect of 0.16 M NaCl added upon the completion of the recording of the lower trace.

lipids indicate that the decay of pyrene monomer emission is multiexponential (Kinnunen et al., 1986). The values measured with the phase demodulation technique thus represent averages over the component lifetimes and must hence be regarded as apparent. However, this jeopardizes neither the qualitative results nor the conclusions of this study. Although longer lifetimes were observed when oxygen was excluded from the cuvette compartment, the qualitative results were essentially identical with those obtained in the presence of oxygen. Therefore, any influence by possible lipid peroxidation does not seem to interfere and was not concerned further. All measurements were done in the presence of atmospheric oxygen.

RESULTS

Requirement of Acidic Phospholipid for the Binding. In preliminary experiments the necessity of acidic phospholipids for the binding of cyt *c* to liposomes could be reconfirmed, Figure 1. As a function of increasing [cyt *c*], progressive quenching of the intensity of pyrene fluorescence at 377 nm due to resonance energy transfer to the heme of cyt *c* is evident when the liquid-crystalline egg PC membrane contains 20 mol % of egg PA. According to the ionic nature of the binding of cyt *c* to the membrane, the decrease in the fluorescence intensity was reversed by the inclusion of 0.16 M NaCl. The decrease by approximately 5% in pyrene emission in the absence of PA is likely to result from trivial absorption as well as from nonspecific adsorption of cyt *c* to the membrane. In order to avoid interference due to these processes, we used instead of steady-state intensity measurements the decrease in the apparent lifetime τ of pyrene monomer fluorescence to monitor the efficiency of energy transfer. This approach has been employed earlier by Vanderkooi et al. using time-correlated photon counting and an anthroyl fatty acid probe as a donor (Vanderkooi et al., 1973). In Figure 2 is illustrated the dependency of τ of PPDPC on the content of egg PA in egg PC liposomes. Clearly, a critical charge density is required, and thus very little binding is observed below 5 mol % of egg PA. Increasing the concentration of egg PA in the membrane causes τ to decrease progressively until at 30 mol % an apparent saturation is reached. Inclusion of 0.4 M NaCl did return τ close to the value measured in the absence of cyt *c*.

Comparison of the Fluorescent Probes. The acidic phospholipids PPHPA and PPDPA were approximately 5% more efficiently quenced by cyt *c* than the corresponding phosphatidylcholine derivatives. This can be expected as the negatively charged polar head group of the PA's should be directly involved in providing a membrane binding site for the

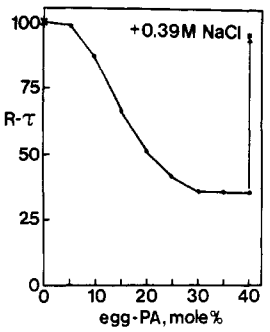

FIGURE 2: Decrease in the average lifetime τ of pyrene monomer fluorescence of PPDPC as a function of content of egg PA in egg PC liposomes. The concentration of cyt c was 3.2 μM, and the lifetime of PPDPC in the absence of egg PA was 100 ± 5 ns. The arrow represents the effect of 0.39 M NaCl on τ in the presence of 40 mol % egg PA.

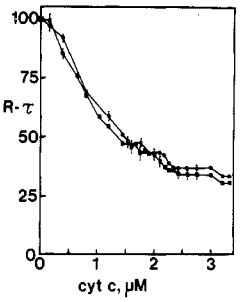

FIGURE 3: Average relative fluoresence lifetime of PPHPC as a function of cyst c concentration. The content of egg PA in the small unilamellar egg PC liposomes was either 30 (●) or 50 mol % (■). The corresponding initial lifetimes were 103 ± 3 and 108 ± 3 ns.

cytochrome. The quenching of the pyrene–phosphatidylcholine lipids is likely to result from the close proximity of heme to the pyrene moiety, occurring as a consequence of the attachment of cyt c to the membrane surface. On the other hand, part of the pyrene–phosphatidylcholines may also be constituting directly to the cyt c binding site in the membrane. No significant differences were seen between the pyrenylhexanoyl and pyrenyldecanoyl lipids as donors although the distance between the membrane surface and the fluorescent moiety is about 5 Å less for the former lipid. This could be related to the observation that the orientation of the pyrene moiety in Langmuir–Blodgett films of PPHPC and PPDPC on cadmium arachidate coated quartz glass slides is different (Kinnunen et al., 1986). In experiments described here, qualitatively identical results were obtained with PPHPC, PPDPC, and PPDPA as quantum donors.

Characteristics of Binding of Cyt c to Liquid-Crystalline Liposomes. With egg PC–egg PA liposomes, τ vs. [cyt c] was measured at egg PA concentrations of 30 and 50 mol %, Figure 3. An apparent saturation in the decrease in τ was first observed at approximately 1.8 μM cyt c. Between 2.0–2.15 and at 3.0 μM cyt c two further stepwise decrements in τ occurred. Similar behavior was evident in the binding of cyt c to liposomes containing either 30 or 50 mol % egg PA, indicating that the number of negatively charged binding sites formed by the acidic phospholipid in the membrane was not limiting. Inclusion of NaCl caused the fluorescence signal to return to values similar to those measured in the absence of cyt c.

Stepwise decreasing of τ as a function of increasing [cyt c] was observed for both uni- and multilamellar egg PC–egg PA liposomes, Figure 4, yet the degree of quenching is significantly larger for the unilamellar vesicles. This can be expected as more than half of the fluorescent probe PPDPA should reside

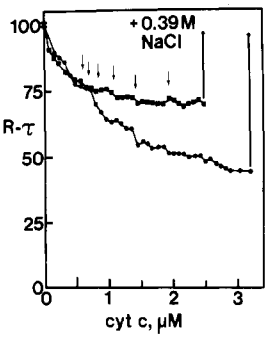

FIGURE 4: Comparison of the binding of cyt c to uni- (●) and multilamellar (■) liposomes of egg PC containing 20 mol % of egg PA and 1 mol % of the probe, PPDPA. Initial τ values in the absence of cyt c were 98 ± 1 and 105 ± 1 ns, for uni- and multilamellar liposomes, respectively. The upward-pointing arrows on the right illustrate the effect of displacement of cyt c from the liposomes by 0.39 M NaCl. Small arrows above the upper trace show the critical [cyt c]/[phospholipid] values predicted by the model presented under Discussion.

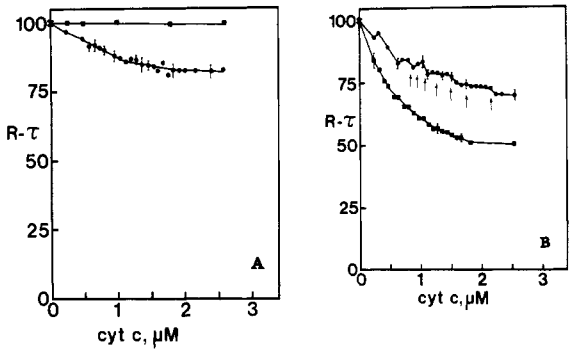

FIGURE 5: (A) Effect of phospholipid phase transition on the binding of cyt c to DPPC liposomes. Content of egg PA was 4 mol %, and the probe was PPDPA. Values for τ were measured as a function of [cyt c] at 15 (●) and 44 °C (■). Without cyt c, the corresponding initial τ values were 98 ± 1 and 54 ± 1 ns, respectively. (B) Comparison of the binding of cyt c to DPPC liposomes below [15 °C (■)] and above [44 °C (●)] the phase transition temperature of this lipid. The content of egg PA was 9 mol %, and the probe was PPDPA. In the absence of cyt c the initial lifetimes at the above temperatures were 100 ± 2 and 51 ± 1 ns, respectively. Arrows beneath the upper trace show the critical [cyt c]/[phospholipid] values obtained from the model forwarded under Discussion.

in the outer monolayer of the membrane of the unilamellar vesicles and thus be available for efficient quenching by membrane-associated cyt c. Only approximately 10% of the lipid molecules are generally estimated to reside in the outermost monolayer of multilamellar liposomes. The signals from both uni- and multilamellar liposomes were stable for at least 1 h, thus suggesting that the structure of the lipid lamellae remains relatively unaltered by cyt c and that cyt c does not translocate in any significant extent through the bilayers as this would finally lead to a similar degree of decrease in τ in both types of liposomes. After the inclusion of 0.4 M NaCl, return of τ to values identical with those measured at an equal concentration of salt in the absence of cyt c was observed, thus indicating lack of transfer of cyt c through the bilayer.

Effect of Phospholipid Phase Transition. We then studied the binding of cyt c to DPPC liposomes containing 5 mol % of egg PA, Figure 5A. At 44 °C, i.e., above the transition temperature of DPPC, cyt c did not influence τ, thus indicating lack of binding of the protein to the membrane. This confirms, similarly to fluid egg PC membranes with low concentrations of egg PA, that the negative charge density in DPPC membranes above the T_m and containing 5 mol % of PA is too low.

When the same experiment is performed at 15 °C where phase separation of egg PA and DPPC is apt to take place, binding of cyt *c* can be observed. However, in contrast to egg PC–egg PA membranes, the decrease in τ did not exhibit clear stepwise decrements as [cyt *c*] increased. When the DPPC membrane contained 10 mol % of egg PA, binding of cyt *c* was observed both above and below the transition temperature of DPPC, Figure 5B. At 44 °C when the membrane is in liquid-crystalline state, the decrease in τ occurred in steps as a function of increasing [cyt *c*], whereas below the transition temperature no such stepwise decrements in τ vs. [cyt *c*] plots were seen.

Discussion

The lack of binding of cyt *c* to neat phosphatidylcholine liposomes could be reconfirmed in this study. The above data also allow the conclusion that this was the case with both unsaturated and saturated phosphatidylcholine and, for the latter, both below and above the phase-transition temperature. However, the phase transition of DPPC in mixed PC–PA liposomes does have a significant effect on the membrane association of cyt *c*. When the concentration of the negatively charged lipid in the liquid-crystalline membrane is too low to provide a binding site for cyt *c*, phase transition of DPPC into the crystalline state brings about phase separation of the unsaturated egg PA in the membrane into separate domains (Galla & Sackmann, 1975; Massari & Pascolini, 1977; Träuble, 1977), which then appear to provide a high enough surface charge density for the attachment of cyt *c*. Phase transition could thus regulate the membrane binding of cyt *c*. Although this result as such is likely to lack any direct physiological relevance, it is of interest to note that a structural transition in the mitochondrial membranes has been shown to accompany changes in the energization state of these organelles (Hackenbrock, 1977).

The characteristics of binding of cyt *c* to liquid crystalline liposomes appears to be somewhat peculiar. Analysis of the data on the decrease in pyrene monomer fluorescence intensity as a consequence of increasing [cyt *c*], Figure 1, indicates, that the binding of cyt *c* to the membrane does not follow a simple Langmuir absorption isotherm and is not a first-order process (not shown). The amount of membrane-bound cyt *c*, nevertheless, increases monotonically as a function of increasing [cyt *c*]. There are no pronounced stepwise changes in contrast to the corresponding measurements on the apparent pyrene monomer fluorescence lifetime, τ (Figures 3, 4, 5B, and 7), which consistently showed kinks in the τ vs. [cyt *c*] plots. These stepwise decrements in τ occurred at approximately identical cyt *c* concentrations with either 30 or 50 mol % of Egg PA in the membrane, Figure 3, indicating that the surface density of PA was not limiting. Under the experimental conditions of this study changes in membrane "microviscosity" and the rate and mode of pyrene excimer formation in addition to the rate of energy transfer to cyt *c* heme are apt to alter the lifetime of the pyrene monomer fluorescence of the probes. Of these three processes, the latter is most closely related to the fluorescence quantum yield and should be less sensitive to factors other than the actual concentration of membrane-bound cyt *c*, which increases monotonously, Figure 1. Therefore, a likely explanation for the observed stepwise decrements in τ vs. [cyt *c*] plots is that in the cyt *c* induced microdomains the membrane microviscosity is changed. In other words, binding of cyt *c* would induce the cooperative formation of microdomains in the membrane, and such membrane should have different "microviscosity" and thus also different τ from the membrane unpertubed by the surface-bound cyt *c*. The shape of the observed curve results from two simultaneous processes, the smoothly decreasing τ due to resonance energy transfer overimposed with the smaller, stepwise changes due to changes in membrane microviscosity. Also, the distribution of the probe as well as the distribution of the other lipids in the membrane could be altered upon the binding of cyt *c*. This would be in accordance with earlier results. Binding of cyt *c* to phosphatidylserine and phosphatidylinositol vesicles containing dansyl-labeled phosphatidylethanolamine causes an increase in fluorescence polarizaton (Faucon et al., 1976). In the experiments performed by these investigators, stepwise changes in the emission anisotropy upon increasing [cyt *c*] are also evident. Vanderkooi et al. reported the monoexponential fluorescence decay kinetics of an anthroyl fatty acid probe in mixed liposomes to become biexponential in the presence of membrane-bound cyt *c*, thus indicating the probe to become redistributed into two different environments (Vanderkooi et al., 1973). Brown and Wütrich, on the other hand, reported on the formation of microdomains of surface-immobilized boundary lipids, directly involved in the binding of cyt *c* to the membrane and forming the actual binding site (Brown & Wütrich, 1977b).

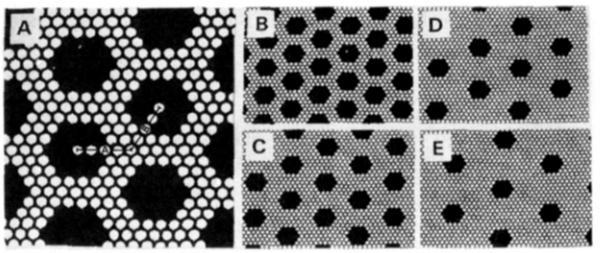

FIGURE 6: Illustration of the two-dimensional n_A/n_B coordinate system (panel A) used for a membrane with a trigonal symmetry for the phospholipid acyl chains. Distances are given as integers and represent the number of translation steps on the lattice coordinate axes. Each dot represents one acyl chain of a phospholipid. One cyt *c* binding site in the membrane is composed of a hexagon formed by 19 acyl chains belonging to 9.5 phospholipids. In the figure $n_A = n_B = 4$, and thus the area per cyt *c* = 48. Panels B–E illustrate four different patterns for the organization of cytochrome *c* on the liposome surface. The coordinates n_A/n_B in these panels are (B) 4/4, (C) 5/5, (D) 6/6, and (E) 7/7, which further correspond to the calculated [cyt *c*]/[accessible lipid] ratios (nmol/μmol) of 41.7, 26.7, 18.5, and 13.6, respectively. See Discussion and Table I for details.

However, the formation of microdomains cannot alone explain the present data as in this case τ would be decreasing monotonously as a function of increasing [cyt *c*], similarly to the measurements on pyrene monomer steady-state fluorescence intensity. This does not apply if these microdomains further arrange in a cooperative manner into distinct, regular two-dimensional arrays with a characteristic lipid distribution (which should depend on the surface density of cyt *c* in a stoichiometric manner) and microviscosity and, accordingly, a characteristic τ value for the accommodated probe. The formation of such microdomains appears to require the membrane to be in a fluid, liquid-crystalline state. Thus, in the experiments using mixed egg PA–DPPC liposomes at a temperature below T_m for the latter lipid no clear stepwise decrements in τ were evident.

The Model. To interpretate the present experimental results, we formulated a model, illustrated in Figure 6 and given in a numerical form in Table I. The model is based on the following assumptions. (i) The acyl chains of those phospholipids anchoring cyt *c* to the membrane surface as well as the acyl chains of the lipids in the remaining liquid-crystalline membrane are hexagonally arranged (Ruocco & Shipley, 1982; Somerharju et al., 1985). (ii) Each surface-immobilized microdomain underneath a bound cyt *c* molecule consists of

Table I: Calculation of Surface Density of Cyt *c* on the Basis of Lattice Coordinates Predicted by the Model[a]

n_A/n_B	area/cyt *c* $(c_A^2 + n_A n_B + n_B^2)$[b]	cyt *c*/lipid (nmol/μmol)[c]	normalized values[d]					
2/3	19	105	1					
3/3	27	74	0.7	1				
3/4	37	54	0.51	0.73	1			
4/4	48	41.7	0.39	0.56	0.77	1		
4/5	61	32.8	0.31	0.44	0.61	0.79	1	
5/5	75	26.7	0.25	0.36	0.49	0.64	0.81	1
5/6	91	22.0	0.21	0.30	0.41	0.53	0.67	0.82
6/6	108	18.5	0.18	0.25	0.34	0.44	0.56	0.69
6/7	127	15.7	0.15	0.21	0.29	0.38	0.48	0.59
7/7	147	13.6	0.13	0.18	0.25	0.33	0.41	0.51
7/8	169	11.8	0.11	0.16	0.22	0.28	0.36	0.44
8/8	192	10.4	0.10	0.14	0.19	0.25	0.32	0.39

[a] See Figure 6 and Discussion for further details. [b] Surface area is given as the number of the lattice phospholipid acyl chains. [c] Lipid refers here to the amount of phospholipid residing in the outermost layer of the liposomes and participating in cyt *c* binding. Numbers in this column were derived as the reciprocal of $(n_A^2 + n_A n_B + n_B^2)/2$ (=number of phospholipids per cyt *c*), which was further multiplied by 1000 to obtain the values in nanomoles of cyt *c* per micromole of lipid. [d] These normalized values give the scales of the different *relative* cyt *c* lattice densities on the membrane surface. The scales were obtained by assigning a given surface concentration of cyt *c* to one, whereafter the less dense patterns are given as fractions thereof.

a hexagon of the 19 acyl chains of 9.5 phospholipids. Previously, the displacement by an embedded protein of a hexagon of acyl chains has been used in the analysis of the distribution of intrinsic membrane proteins (Pink et al., 1984). (iii) We further assume that in all cases the facets of the hexagons are parallel, Figure 6. Accordingly, the distance between the individual membrane-associated cyt *c*'s can then be given as integers n_A and n_B, representing the number of translation steps of lipid acyl chains between the centers of the microdomains, Figure 6. It follows that discrete values for the realized surface densities of cyt *c* should exist, in turn corresponding to specific bulk molar ratios of the constituents. It is easily shown that by use of the surface area per acyl chain as a unit the area of membrane available per one molecule of cyt *c* is given by $n_A^2 + n_A n_B + n_B^2$. (iv) The affinity of cyt *c* toward acidic phospholipids is very high with a dissociation constant of approximately 1–3 μem cyt *c* (Nicholls, 1974; Teissie & Baundras, 1977). Due to the number of uncertainties involved, we have not tried to correct for the fraction of cyt *c* free in solution but have assumed for the sake of simplicity all protein to become associated with the membrane. (v) There is no major asymmetry in the distribution of lipids between the inner and outer leaflets of the bilayer.

Table I summarizes the different predicted patterns that cyt *c* can form on the membrane surface, represented as integer values for n_A and n_B. Also given are the corresponding areas per cyt *c* as a number of membrane phospholipid acyl chains. These values are further converted to cyt *c*/lipid molar ratios, where the amount of lipid stands for those lipid molecules present in the outermost monolayer of the liposomes and thus accessible for cyt *c* binding. Normalized values are then obtained by setting the highest [cyt *c*]/[lipid] value (representing the most dense binding pattern for the different cases) to one and relating the rest of the predicted values to this to obtain a relative scale for an easy analysis of the experimental data.

The model was then applied to the experimental results shown in Figures 4, 5B, and 7. This comparison is summarized in Table II. To vary the amount of lipid in the outermost monolayer of the liposomes, different sonication techniques were used to produce, tentatively, (a) large multilamellar, (b) "intermediate multilamellar", and (c) small unilamellar vesicles. We then normalized the highest observed critical cyt *c*/phospholipid molar ratio (evident as a stepwise decrement in τ) to one, whereafter the rest of the critical values were taken from the experimental data and transformed to the

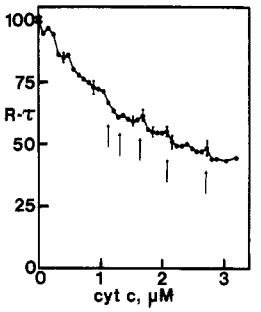

FIGURE 7: Decrease in the average relative fluorescence lifetime of PPDPA as a function of [cyt *c*]. The content of egg PA in multilamellar liposomes was 20 mol %. The initial value for τ was 103 ± 4 ns. The highest observed critical cyt *c* concentration of 2.92 μM was normalized to one (the arrow on the right). Comparison of the normalized observed values with the scales in Table I indicates the highest observed critical cyt *c* concentration to correspond to a lattice of $n_A = 4$ and $n_B = 5$. The predicted critical values for [cyt *c*] marked by arrows were then obtained from the model. To produce liposomes intermediate in size between multi and unilamellar and prepared by bath and probe sonication, respectively, a horn-type sonicator was used.

Table II: Comparison of Experimental Data with the Model[a]

	data from Figure		
	4[b]	7[c]	5B[d]
highest obsd critical [cyt *c*] (μM)	1.92	2.72	2.16
normalized to one[e]	1.00 (1.00)	1.00 (1.00)	1.00 (1.00)
rest of the obsd, normalized critical [cyt *c*] values	0.71 (0.73)	0.77 (0.77)	0.81 (0.82)
	0.50 (0.56)	0.62 (0.61)	0.67 (0.69)
	(0.44)	0.50 (0.49)	0.59 (0.59)
	0.38 (0.36)	(0.41)	0.49 (0.51)
	0.29 (0.30)	0.38 (0.34)	(0.44)
			0.37 (0.39)
highest obsd. [cyt *c*] corresponds to n_A and n_B of	3/3	3/4	5/5
calcd concn of accessible lipid (μM)[f]	25.9	50.4	80.9
percent of total lipid[g]	13	25.2	40.4

[a] See discussion for further details. [b] Liposomes prepared by a bath sonicator. [c] Liposomes prepared by a horn sonicator. [d] Liposomes prepared by a probe sonicator. [e] Numbers in parentheses give the corresponding normalized scale, taken from Table I. [f] These numbers were obtained by dividing the highest observed critical [cyt *c*] by the corresponding cyt *c*/lipid molar ratio to yield the lipid concentration in the outermost layer of the liposomes. [g] The lipid in the outermost layer liposomes as a percent of the total, 0.2 mM lipid.

relative scale. These experimental normalized values were subsequently compared with the theoretical scales of normalized values of Table I, and best fits were observed. On this basis, by starting from the coordinates and the known concentration of cyt *c*, the amount of lipid in the outermost monolayer could be calculated. The predictive value of the model appears to be rather good. Yet, it is to be emphasized that we are merely trying to offer an explanation to our experimental results. Therefore, this agreement does not warrant the model to be correct, and other explanations may certainly be equally applicable.

The above model for a regular surface distribution of cyt *c* in liposomes necessitates lipid-mediated long-range order to prevail in liposomal membranes and that ordering can be induced by extrinsic membrane proteins. Due to theoretical considerations, Jähnig has proposed the range of intrinsic membrane protein induced ordering in membranes to be ca. 15 Å (Jähnig, 1981). However, recent experimental data for bacteriorhodopsin reconstituted in dimyristoylphosphatidylcholine does reveal the range of lipid-mediated, intrinsic membrane protein induced order to be considerably longer, in this case exceeding 45 Å (Rehorek et al., 1985). Similarly to the experiments by Rehorek et al., we are by large observing fluorescence from those pyrene lipids residing at a distance larger than the critical range of Förster energy transfer from the pyrene probe to cyt *c*.

As to the underlying physical principles causing the formation of regular membrane alloys, there is some analogy to the characteristics of adatom structures on single-crystal substrate surfaces where a remarkably high degree of long-range order is often observed (Clarke, 1985). It has been proposed that perturbation of the substrate electron densities by the adsorbate atoms may result in an "indirect" interaction via substrate due to the adatoms causing long-range oscillatory fluctuations in the substrate electron densities, thus explaining the specific patterns of adlayers formed as a function of substrate coverage (Einstein & Schrieffer, 1973). Incorporation of intrinsic proteins into biomembranes has been shown to cause low-frequency motions in the membrane to become more intense (Kang et al., 1979; Paddy et al., 1981; Cornell et al., 1982). Such low-frequency oscillations should produce long-range correlations in the membrane and have been suggested to play a significant role in information and energy transfer in biological membranes (Fröhlich, 1980; Cornell et al., (1982). The present results also suggest the possibility that changes in the long-range order in biomembranes could be induced by peripheral membrane proteins and therefore probably by other ligands such as hormones as well. Lateral diffusion coefficients for certain fluorescent lipid probes in the hepatocyte plasma membranes were reduced by 20–30% by insulin whereas no effect on fluorescently labeled proteins was observed (Stuschke & Bojar, 1985).

To this end, it is of interest that macroscopic phase separation in monolayers of binary lipid mixtures with fluorescent probes can be directly observed as crystalline structures visible in fluorescence microscopy (Lösche et al., 1983, 1984; Lösche & Möhwald, 1984; Peters & Beck, 1983; Fischer et al., 1984; McConnell et al., 1984; Weis & McConnell, 1984). These structures pack in monolayer films in patterns indicating the involvement of stabilizing forces with trigonal symmetry elements. This formation of two-dimensional crystallites in binary lipid mixtures reveals the presence of macroscopic long-range correlations in the lipid monolayers. There is no a priori reason to assume lipids in liposomal bilayers to be distinctly less organized except that due to restrictions imposed by their smaller surface area and factors relating to molecular geometries and surface curvature (Israelachvili et al., 1980).

Registry No. Cytochrome *c*, 9007-43-6; dipalmitoylphosphatidylcholine, 2644-64-6.

References

Birrell, G. B., & Griffith, O. H. (1976) *Biochemistry 15*, 2925–2929.

Brown, L. R., & Wütrich, K. (1977a) *Biochim. Biophys. Acta 464*, 356–369.

Brown, L. R., & Wütrich, K. (1977b) *Biochim. Biophys. Acta 468*, 389–410.

Chapman, D., & Urbina, J. (1971) *FEBS Lett. 12*, 169–172.

Clarke, L. J. (1985) *Surface Crystallography*, Wiley-Interscience, New York.

Cornell, B. A., Davenport, J. B., & Separovic, F. (1982) *Biochim. Biophys. Acta 689*, 337–345.

Davidson, F. M., & Long, C. (1958) *Biochem. J. 69*, 458–466.

Einstein, T. L., & Schreiffer, J. R. (1973) *Phys. Rev. B: Solid State 7*, 3629–3648.

Faucon, J. F., Dufourcq, J., Lussan, C., & Bernon, R. (1976) *Biochim Biophys. Acta 435*, 283–294.

Fischer, A., Lösche, M., Möhwald, H., & Sackmann, E. (1984) *J. Phys. Lett. 45*, *l785*–L791.

Fröhlich, H. (1980) *Adv. Electron. Electron Phys. 53*, 85–152.

Fromherz, P. (1970) *FEBS Lett. 11*, 205–208.

Galla, H.-J., & Sackmann, E. (1975) *Biochim. Biophys. Acta 401*, 509–529.

Galla, H-J., & Hartmann, W. (1980) *Chem. Phys. Lipids 27*, 199–219.

Green, D. E., & Fleischer, S. (1963) *Biochim. Biophys. Acta 70*, 554–584.

Hackenbrock, C. (1977) in *Structure of Biological Membranes* (Abrahamsson, S., & Pascher, I., Eds.) pp 199–234, Plenum, New York.

Israelachvili, J. N., Marcelja, S., & Horn, R. G. (1980) *Q. Rev. Biophys. 13*, 121–200.

Jähnig, F. (1981) *Biophys. J. 36*, 329–357.

Kang, S. Y., Gutowsky, H. S.; Hsung, J. C., Jacobs, R., King, T. E., Rice, D., & Oldfield, E. (1979) *Biochemistry 18*, 3257–3267.

Kimelberg, H. K., & Lee, C. P. (1969) *Biochem. Biophys. Res. Commun. 34*, 784–790.

Kimelberg, H. K., & Papahadjopoulos, D. (1971) *J. Biol. Chem. 246*, 1142–1148.

Kinnunen, P. K. J., Virtanen, J. A., Tulkki, A. P., Ahuja, R., & Möbius, D. (1986) *Thin Solid Films 132*, 193–203.

Lakowicz, J. R., Cherek, H., & Balter, A. (1981) *J. Biochem. Biophys. Methods 5*, 131–146.

Lösche, M., & Möhwald, H. (1984) *Eur. Biophys. J. 11*, 35–42.

Lösche, M., Sackmann, E., & Möhwald, H. (1983) *Ber. Bunsen-Ges. Phys. Chem. 87*, 848–852.

Lösche, M., Rabe, J., Fischer, A., Rucha, B. U., Knoll, W., & Möhwald, H. (1984) *Thin Solid Films 117*, 269–280.

Massari, S., & Pascolini, D. (1977) *Biochemistry 16*, 1189–1195.

McConnell, H. M., Tamm, L. K., & Weis, R. M. (1984) *Proc. Natl. Acad. Sci. U.S.A. 81*, 3249–3253.

Nicholls, P. (1974) *Biochim. Biophys. Acta 346*, 261–310.

Nicholls, P., & Malviya, A. N. (1973) *Trans Biochem. Soc. 1*, 372–375.

Paddy, M. R., Dahlquist, F. W., Davis, J. H., & Bloom, M. (1981) *Biochemistry 20*, 3152–3162.

Peters, R., & Beck, K. (1983) *Proc. Natl. Acad. Sci. U.S.A. 80*, 7183–7187.

Pink, D. A., Chapman, D., Laidlaw, D. J., & Wiedmer, T. (1984) *Biochemistry 23*, 4051–4058.
Pohl, W. G., & Teissie, J. (1975) *Z. Naturforsch C: Biosci. 30C*, 147–151.
Quinn, P. J., & Dawson, R. M. C. (1969) *Biochem. J. 115*, 65–75.
Rehorek, M., Dencher, N. A., & Heyn, M. P. (1985) *Biochemistry 24*, 5980–5988.
Ruocco, M. J., & Shipley, G. G. (1982) *Biochim. Biophys. Acta 691*, 309–320.
Singleton, W. S., Gray, M. S., Brown, M. L., & White, J. L. (1965) *J. Am. Oil Chem. Soc. 42*, 53–61.
Somerharju, P. J., Virtanen, J. A., Eklund, K., Vainio, P., & Kinnunen, P. K. J. (1985) *Biochemistry 24*, 2773–2781.
Spencer, R. D., & Weber, G. (1970) *J. Chem. Phys. 52*, 1654–1663.
Steinemann, A., & Läuger, P. (1971) *J. Membr. Biol. 4*, 74–86.
Stuschke, M., & Bojar, H. (1985) *Biochim. Biophys. Acta 845*, 436–444.
Sunamoto, J., Kondo, H., Nomura, T., & Okamoto, H. (1980) *J. Am. Chem. Soc. 102*, 1146–1152.
Teissie, J. (1981) *Biochemistry 20*, 1554–1560.
Teissie, J., & Baudras, A. (1977) *Biochimie 59*, 693–703.
Thurén, T., Vainio, P., Virtanen, J. A., Blomqvist, K., Somerharju, P. J., & Kinnunen, P. K. J. (1984) *Biochemistry 23*, 5129–5134.
Träuble, H. (1977) in *Structure of Biological Membranes* (Abrahamsson, S., & Pascher, I., Eds.) pp 509–550, Plenum, New York.
Van, S. P., & Griffith, O. H. (1975) *J. Membr. Biol. 20*, 155–170.
Vanderkooi, J., Erecinska, M., & Chance, B. (1973) *Arch. Biochem. Biophys. 154*, 219–229.
Weis, R. M., & McConnell, H. M. (1984) *Nature (London) 310*, 47–49.

Characterization of Hyaluronate Binding Proteins Isolated from 3T3 and Murine Sarcoma Virus Transformed 3T3 Cells†

E. A. Turley,*,‡ D. Moore,‡ and L. J. Hayden§

Division of Oncology, Department of Pharmacology, and Division of Endocrinology, Department of Pharmacology, The University of Calgary, Calgary, Alberta, Canada T2N 4N1

Received June 23, 1986; Revised Manuscript Received December 8, 1986

ABSTRACT: A hyaluronic acid binding fraction was purified from the supernatant media of both 3T3 and murine sarcoma virus (MSV) transformed 3T3 cultures by hyaluronate and immunoaffinity chromatography. Sodium dodecyl sulfate–polyacrylamide gel electrophoresis resolved the hyaluronate affinity-purified fraction into three major protein bands of estimated molecular weight ($M_{r,e}$) 70K, 66K, and 56K which contained hyaluronate binding activity and which were termed hyaluronate binding proteins (HABP). Hyaluronate affinity chromatography combined with immunoaffinity chromatography, using antibody directed against the larger HABP, allowed a 20-fold purification of HABP. Fractions isolated from 3T3 supernatant medium also contained additional binding molecules in the molecular weight range of 20K. This material was present in vanishingly small amounts and was not detected with a silver stain or with [^{35}S]methionine label. The three protein species isolated by hyaluronate affinity chromatography ($M_{r,e}$ 70K, 66K, and 56K) were related to one another since they shared antigenic determinants and exhibited similar p*I* values. In isocratic conditions, HABP occurred as aggregates of up to 580 kilodaltons. Their glycoprotein nature was indicated by their incorporation of ^{3}H-sugars. Enzyme-linked immunoadsorbent assay showed they were antigenically distinct from other hyaluronate binding proteins such as fibronectin, cartilage link protein, and the hyaluronate binding region of chondroitin sulfate proteoglycan. The apparent dissociation constant of HABP for hyaluronate was approximately 10^{-8} M, and kinetic analyses showed these binding interactions were complex and of a positive cooperative nature. Tryptic peptide fingerprinting and immunological cross-reactivity suggested the HABP from the virally transformed and the parent cell line sources were closely related. Nevertheless, structural differences were demonstrated by distinct p*I* values and unique peptide sequences. These results are discussed with regard both to the functional significance of hyaluronate–cell surface interactions in transformed as well as normal cells and to the relationship of HABP to other reported hyaluronate binding proteins.

Hyaluronate is one of several glycosaminoglycans that has been implicated in regulating cell behavior during tumorigenesis and embryogenesis (Toole, 1982). Thus, production of hyaluronate is elevated during the morphogenesis of a variety of embryonic tissues (Toole, 1982), in tumor variants selected for enhanced metastatic/invasive capability (Kimata et al., 1983; Turley & Tretiak, 1985), and at the site of invasion of tumors into host tissue (Toole et al., 1979; Kupchella & Baki-Hashemi, 1982; Turley & Tretiak, 1985). Hyaluronate has profound effects on cell behavior in vitro that may contribute to developmental and disease states such as cell overlapping (Turley, 1982), morphology (Toole, 1982), motility (Culp, 1976; Turley & Torrance, 1985), adhesion, and immunogenicity (Toole, 1982). Furthermore, it affects the

† Supported by a Medical Research Council grant, a National Cancer Institute of Canada scholarship to E.A.T., and an Alberta Cancer Board grant to L.J.H.

* Address correspondence to this author.
‡ Division of Oncology, Department of Pharmacology.
§ Division of Endocrinology, Department of Pharmacology.

0006-2960/87/0426-2997$01.50/0